

Bifurcations as dissociation mechanism in bichromatically driven diatomic molecules

S. Huang^{1,*}, C. Chandre², and T. Uzer¹

¹ *Center for Nonlinear Science, School of Physics,*

Georgia Institute of Technology, Atlanta, Georgia 30332-0430, U.S.A.

² *Centre de Physique Théorique[†], Luminy - case 907, 13288 Marseille cedex 09, France*

(Dated: November 11, 2018)

Abstract

We discuss the influence of periodic orbits on the dissociation of a model diatomic molecule driven by a strong bichromatic laser fields. Through the stability of periodic orbits we analyze the dissociation probability when parameters like the two amplitudes and the phase lag between the laser fields, are varied. We find that qualitative features of dissociation can be reproduced by considering a small set of short periodic orbits. The good agreement with direct simulations demonstrates the importance of bifurcations of short periodic orbits in the dissociation dynamics of diatomic molecules.

PACS numbers: 82.50.Pt, 82.50.Nd, 82.20.Nk, 05.45.Gg

[†] UMR 6207 of the CNRS, Aix-Marseille and Sud Toulon-Var Universities. Affiliated with the CNRS Research Federation FRUMAM (FR 2291). CEA registered research laboratory LRC DSM-06-35.

*Electronic address: gtg098n@mail.gatech.edu

I. INTRODUCTION

The dissociation behavior of molecules driven by bichromatic fields with commensurate frequencies has emerged as a rich research subject, especially for the control of molecular processes [1, 2]. The interplay of the two radiation fields opens up many new dissociation pathways, and it is well known that the relative phase between the two fields can affect these pathways drastically, so much so that the relative phase can be used as a means to control the outcome of the reaction [3, 4]. However, the mechanisms by which the relative phase controls the dissociation behavior are less well-known. The relative phase is a very convenient control parameter since it does not require additional energy input from the fields (as opposed to their amplitudes).

The two-color laser-driven dissociation of molecules is also of great interest to researchers because these seemingly simple systems display complex dynamics and behavior that single component laser field cannot exhibit [1, 2, 3, 4, 5, 6, 7, 8, 9]. The theoretical literature on laser-driven dissociation of molecules has been extensive in the past three decades [3, 4, 5, 6, 7, 8, 9, 10, 11, 12, 13, 14, 15, 16, 17, 18, 19, 20]. Among these is Ref. [7] where the dissociation probability of a model diatomic molecule exposed to a two-color laser field was investigated for various parameters using direct simulations of the classical-mechanical equations.

In this paper, we report how the dissociation probability obtained in Ref. [7] by direct numerical simulations can be understood qualitatively using a linear stability analysis of a small set of periodic orbits. Our main result is that for most parameter values the principal features of the dissociation probability can be reproduced using two short periodic orbits (with the period equal to the one of the fields), and in particular by the identification of

the main bifurcations which have a drastic effect on the dissociation probability. In this way, our approach allows the qualitative prediction, with significant time savings, of the dynamics as parameters are varied. Indeed, the typical time necessary for the computation of a periodic orbit and its stability is of the order of its period which is also the period of the field. Our findings echo similar ones obtained in the microwave ionization of Rydberg atoms in a strong bichromatic field for which qualitative agreement has been obtained with experimental data and a quantitative agreement with quantal simulations [21].

After describing the model in Sec. II, we briefly summarize the method which monitors the position and the residue of periodic orbits [22] in Sec. III. In Sec. IV, we analyze the dynamics using a selection of short periodic orbits, as parameters are varied in Sec. IV A. We relate a linear stability measure (the residue of a given periodic orbit) to the dissociation probability in Sec. IV B. Good agreement is found for most parameter values. A discrepancy is observed for small phases and is discussed in Sec. IV C.

II. THE MODEL

The Hamiltonian (in atomic units) of a diatomic molecule exposed to a strong bichromatic field with a phase lag can be modeled as

$$\begin{aligned}
 H(r, p, \tau) = & \frac{p^2}{2m} + D [1 - e^{-\alpha(r-r_e)}]^2 \\
 & + (r - r_e)[A_1 \sin(\Omega_1 \tau) + A_2 \sin(\Omega_2 \tau + \phi)],
 \end{aligned} \tag{1}$$

where the parameters are the reduced mass m , the dissociation energy D , and the equilibrium distance r_e . Here we assume that the envelopes of the pulses are constant since the pulse duration has a very minor impact on this system, as suggested in Ref. [7]. The relevant dimensionless variables are $\tilde{r} = \alpha(r - r_e)$, $\tilde{p} = p/\sqrt{2Dm}$, $t = \alpha\sqrt{2D/m}\tau$, $F_i = A_i/(2D\alpha)$,

$\omega_i = \Omega_i / \sqrt{2D\alpha^2/m}$. In these new coordinates, the Hamiltonian (1) is

$$\begin{aligned} \tilde{H}(\tilde{r}, \tilde{p}, t) = & \frac{\tilde{p}^2}{2} + \frac{1}{2} (1 - e^{-\tilde{r}})^2 \\ & + \tilde{r} (F_1 \sin \omega_1 t + F_2 \sin(\omega_2 t + \phi)), \end{aligned} \quad (2)$$

where \tilde{r} and \tilde{p} are canonically conjugate.

In what follows, we model the hydrogen fluoride (HF) molecule in which $m = 1732$, $D = 0.2101$, $r_e = 1.75$ and $\alpha = 1.22$ (all in atomic units.) We consider a field with two commensurate frequencies such that $\omega_1 = \omega_2/3 = 0.28$. We notice that Hamiltonian (2) is time-periodic with period $2\pi/\omega_1$.

III. RESIDUE METHOD

The general idea of the residue method is to follow a set of periodic orbits as parameters are varied in order to determine qualitative properties of the dynamics. As it was shown in other, similar problems, short periodic orbits play the role of organizing centers for the dynamics [21, 23, 24]. Higher-order periodic orbits give more refined details of the dynamics, especially on longer time scales. In principle, for atomic and molecular systems where short pulses are considered, only short periodic orbits should influence the dynamics. We determine the location of a periodic orbit (given by its number of intersections with the apt Poincaré surface of section) using a modified Newton-Raphson multi-shooting algorithm as described in Ref. [25]. The initial conditions from which the Newton map are iterated is determined in two possible ways : By a quick inspection of the Poincaré section (which is easier if the periodic orbit is elliptic since it shows resonant islands around the periodic orbit considered) or by continuation of periodic orbits for other values of parameters (which is clearly the optimal way since periodic orbits usually deform continuously as parameters are

varied, and even bifurcate). We also monitor the linear stability properties of these periodic orbits which are obtained by integrating the reduced tangent flow along the periodic orbit

$$\frac{d\mathcal{J}^t}{dt} = \mathbb{J} \nabla^2 \tilde{H}(\tilde{r}, \tilde{p}, t) \mathcal{J}^t,$$

where $\mathbb{J} = \begin{pmatrix} 0 & 1 \\ -1 & 0 \end{pmatrix}$ and $\nabla^2 \tilde{H}$ is the two-dimensional Hessian matrix (composed of second derivatives of \tilde{H} with respect to its canonical variables \tilde{r} and \tilde{p}). The initial condition is $\mathcal{J}^0 = \mathbb{I}_2$ (the two-dimensional identity matrix). For a periodic orbit with period T where $T = 2\pi n/\omega_1$ (n being the number of intersections with the Poincaré section), the two eigenvalues of the monodromy matrix \mathcal{J}^T (which make the pair $(\lambda, 1/\lambda)$) determine the stability properties. The determinant of \mathcal{J}^T is equal to 1 since the flow is volume preserving. If the spectrum is $(e^{i\omega}, e^{-i\omega})$, the periodic orbit is elliptic (stable, except in some rare cases); or hyperbolic if the spectrum is $(\lambda, 1/\lambda)$ with $\lambda \in \mathbb{R}^*$ (unstable). Through the use of Greene's residue R [26, 27]

$$R = \frac{2 - \text{tr} \mathcal{J}^T}{4},$$

the stability properties can be deduced in a concise form. If $R \in]0, 1[$, the periodic orbit is elliptic; if $R < 0$ or $R > 1$ it is hyperbolic; and if $R = 0$ and $R = 1$, it is parabolic.

For a given periodic orbit, we follow its location in phase space and its residue as parameters are varied. There are three parameters in our problem: Two amplitudes F_1 and F_2 , and a phase lag ϕ . We compute $R(F_1, F_2, \phi)$ and identify the points in parameter space where bifurcations occur. We are interested in the bifurcations whenever a periodic orbit is likely to change its linear stability, which occurs in particular for $R(F_1, F_2, \phi) = 0$ or $R(F_1, F_2, \phi) = 1$. In general such bifurcations (based on a linear stability analysis) will also play an important role in the nearby phase space region (by continuity in phase space).

IV. DISSOCIATION PROBABILITY

A. Identification of fundamental periodic orbits

Figure 1 shows a Poincaré section (stroboscopic plot of phase space with period $2\pi/\omega_1$) of Hamiltonian (2) for amplitudes $F_1 = 0.18$, $F_2 = 0.02$ and phase lag $\phi = 0$. We notice that an elliptic island is present at the entrance of the dissociation channel. At the center of this island sits an elliptic periodic orbit with one intersection with the Poincaré surface of section (i.e. with period $2\pi/\omega_1$). Standard Hamiltonian dynamics show that the trajectories that are likely to dissociate can become trapped around the resonant island for a while before finding an escape route. Therefore, this particular periodic orbit, which we call \mathcal{O}_e , plays a crucial role in the dissociation probability, and is the focus of the current paper : We investigate its role as the parameters (F_1, F_2, ϕ) are varied. Due to the symmetry ($\phi \mapsto \pi - \phi$) the fundamental domain of variations of ϕ is $[0, \pi[$. We also restrict the amplitudes to $(F_1, F_2) \in [0, 0.22] \times [0, 0.06]$.

We anticipate two factors which can influence dissociation: One is the location of this orbit, and the other is a change of its stability. In Fig. 2, we represented the position of \mathcal{O}_e or, more precisely, its action and angle variables as defined by [10]

$$I = 2 \left(1 - \sqrt{1 - E} \right),$$

$$\tan \theta = - \frac{\tilde{p} \sqrt{1 - E}}{1 - e^{-\tilde{r}} - E},$$

where $E(\tilde{r}, \tilde{p}) = \tilde{p}^2 + (1 - e^{-\tilde{r}})^2$, for a typical set of parameters $F_1 = 0.18$ and $F_2 = 0.02$, while ϕ is varied. The main conclusion is that the variation of the action and angle of \mathcal{O}_e do not seem to be linked to the variation of the dissociation probability since they do not vary significantly as ϕ is increased. In addition they are not monotonic functions of ϕ in contrast

with the dissociation probability. Hence, the position of the specific periodic orbit does not appear to play a significant role (at least in the range of parameters considered).

The second possible mechanism based on a bifurcation has a more drastic influence on dissociation. In order to monitor this bifurcation properly, we also need to follow the associated hyperbolic orbit [22]. To see an increase of dissociation we need to ensure that the hyperbolic orbit stays hyperbolic while the elliptic one turns hyperbolic (in order to discard a stability exchange which would not affect the dissociation probability significantly). A typical residue plot (the residue as a function of ϕ) is shown in Fig. 3 for $F_1 = 0.18$ and $F_2 = 0.02$. We notice that an increase of ϕ is always associated with an increase of the residue. At $\phi = 0.75$, the residue crosses unity and a bifurcation (which is a period doubling) occurs. This increase of hyperbolicity is associated with increased chaos and hence more dissociation. This is in agreement with the direct simulations of Ref. [7].

We should point out that the computation of Ref. [7] uses initial conditions in the ground state ($E = 0.045$), which is lower than the set of periodic orbits we consider ($E = 0.29$) in Fig. 1. This justifies the importance of the chosen periodic orbits for dissociating trajectories. For other values of parameters we consider, the energy level of the periodic orbit \mathcal{O}_e is always well above $E = 0.045$.

B. Residue contour plots in parameter space

For fixed values of ϕ , we vary the amplitudes F_1 and F_2 and compute the residue values of the periodic orbit \mathcal{O}_e . We depict the contour plots of these residues in Fig. 4 in the (F_1, F_2) plane for $\phi = 0, \pi/6, \pi/2$ and π . These figures should be compared to Fig. 2 of Ref. [7]. In Fig. 4, darker regions represent lower residue values, and hence are expected to reveal more stable dynamics (smaller dissociation probability) for the corresponding parameters.

On these residue contours we have superposed the curves $R(F_1, F_2) = 1$ (white dashed curves) through which the periodic orbit \mathcal{O}_e changes its stability. The corresponding bifurcation from elliptic to hyperbolic linear stability indicates a possible increase in dissociation probability due to an increase of hyperbolicity in this region of phase space. Since the trajectories are no longer trapped when \mathcal{O}_e is hyperbolic, it is expected that the dissociation probability increases. This is in good agreement with Ref. [7] where we notice that for $\phi = \pi/6, \pi/2$ and π , there is a qualitative agreement in the shape of the dissociation probability. In particular, the following features are reproduced for a fixed value of ϕ : the non-monotonicity for $\phi = \pi/6$ as F_2 is increased (with a fixed value of F_1), and the monotonicity for $\phi = \pi/2$ and π with a sharper downward bifurcation curve (dashed line) for $\phi = \pi$ as F_2 is increased in the region $F_2 \in [0, 0.05]$. Our analysis also confirms that the stabilization effect decreases when ϕ is increased (from 0 to π). For $\phi = 0$ case, the contour plot shows agreement with direct simulations for most regions in the (F_1, F_2) plane once more, and the property that it reproduces the two upper-right bumps observed in the dissociation probability contour plot. These are interpreted as remnants of the ellipticity of the bifurcated \mathcal{O}_e . We notice that the corresponding hyperbolic periodic orbit \mathcal{O}_h remains hyperbolic ($R < 0$) for most values of the parameters. However, for $\phi \in [\pi/6, \pi]$, there is a region around the upper-right corner of the (F_1, F_2) plane where the \mathcal{O}_h turns to elliptic and then returns to hyperbolic, as it is shown on the (F_1, F_2) plane contour plot of Fig. 4 (b). In general, this bifurcation does not affect the dissociation probability because, due to its location, it does not play an important role compared to the periodic orbit \mathcal{O}_e which has already bifurcated ($R > 1$) for these parameter values (see Figs. 4 (c) and (d)). However, for low values of ϕ and high values of the amplitudes F_i , the orbit \mathcal{O}_e is still elliptic and \mathcal{O}_h undergoes a bifurcation, as shown in Figs. 7 which we discuss in the following section.

This region corresponds to the disagreement observed for $\phi = 0$ on Fig. 4 with the direct simulations of Ref. [7] to which we turn next.

C. Low values of ϕ : Influence of \mathcal{O}_h

For $\phi = 0$, we observe two branches on Fig. 4 (a) where the residues of \mathcal{O}_e vanish. Along these lines we expect, from a linear stability analysis, locally a constant degree of chaos, and hence dissociation probability. However, this is not seen in direct simulations since the dissociation probability actually increases along these lines as F_2 is increased. This feature is shown using laminar plots which represent contour plots of the number of return times on the Poincaré section before dissociation (defined as trajectories for which E becomes greater than $E_{th} = 2$). The maximum integration time is $200\pi/\omega_1 \approx 2244$. Figure 5 shows laminar plots for the set of parameters on the line of vanishing residues (as F_2 is increased) as marked by crosses in Fig. 4 (a), and Figure 6 represents two additional laminar plots for parameter sets transverse to that line (with a fixed F_2 and increasing F_1), marked by circles in Fig. 4 (a). These plots show clearly that dissociation increases as F_2 is increased. Even locally around the considered periodic orbit \mathcal{O}_e , there seems to be more chaos as F_2 is increased. The situation is more complex at parameter values off the vanishing-residue line as F_1 is varied on Fig. 6 where the overall amount of dissociation seems to be similar but with very different distributions of dissociating trajectories. All these features originate from the nonlinear stability which can be captured by considering the linear stability of higher order periodic orbits around the boundary of the elliptic island \mathcal{O}_e .

For insights into the parameter region where this discrepancy occurs, we describe here the associated bifurcation. In Fig. 7 the residue as a function of F_1 is plotted for both \mathcal{O}_e and \mathcal{O}_h with fixed F_2 and ϕ . We see clearly that there is a loop around $R = 0$, indicating that

\mathcal{O}_h undergoes a bifurcation at $R = 0$ which involves three periodic orbits of the same period, two hyperbolic ones and an elliptic one. When ϕ is equal to 0, the upper part of the loop merges with the residue curve of \mathcal{O}_e , as shown in Fig. 7(b), for which the loop size reaches its maximum size. The following picture emerges : Without a loop in the residue curve, the system has two periodic orbits with the period of the field, \mathcal{O}_e and \mathcal{O}_h . In the region of parameters where there is a loop in the residues, the system has four of these periodic orbits, two elliptic ones (which are close to each other or even coincide at $\phi = 0$) and two hyperbolic ones. This additional hyperbolicity increases chaos (and hence dissociation) locally.

Conclusions

We have analyzed the dissociation dynamics of a model diatomic molecule driven by a bichromatic field in terms of periodic orbit bifurcations. Following the linear stability of a few selected periodic orbits, we reproduced the dissociation probability qualitatively in parameter space (two field amplitudes and one relative phase). For relatively low ϕ and high amplitudes F_i , the original hyperbolic periodic orbit \mathcal{O}_h undergoes a particular bifurcation, which leads to two branch lines on the F_1 - F_2 residue plane. Along these two branch lines, there is a discrepancy between predictions based on the residues and direct simulations. The role of additional periodic orbits is underlined regardless of whether the discrepancy originates from bifurcated orbits (and the resulted increase of hyperbolicity) or from higher-order periodic ones.

Acknowledgments

This research was partially supported by the US National Science Foundation. C.C. acknowledges support from Euratom-CEA (contract EUR 344-88-1 FUA F).

- [1] M. Shapiro and P. Brumer, Rep. Prog. Phys. **66**, 859 (2003).
- [2] R. J. Gordon, L. Zhu and T. Seideman, Acc. Chem. Res. **32**, 1007 (1999).
- [3] V. S. Batista and P. Brumer, Phys. Rev. Lett. **89**, 143201 (2002).
- [4] E. Charron, A. Giusti-Suzor and F. H. Mies, Phys. Rev. A **49**, R641 (1994).
- [5] M. E. Goggin and P. W. Milonni, Phys. Rev. A **38**, 5174 (1988).
- [6] J. R. Stine and D. W. Noid, Opt. Commun. **31**, 161 (1979).
- [7] V. Constantoudis and C. A. Nicolaides, J. Chem. Phys. **122**, 084118 (2005).
- [8] J. Levesque, S. Chelkowski and A. D. Bandrauk, J. Phys. Chem. A **107**, 3457 (2003).
- [9] F. He, C. Ruiz and A. Becker, Phys. Rev. Lett. **99**, 083002 (2007).
- [10] Y. Gu and J.-M. Yuan, Phys. Rev. A **36**, 3788 (1987).
- [11] V. Constantoudis and C. A. Nicolaides, Phys. Rev. E **64**, 056211 (2001).
- [12] V. Constantoudis and C. A. Nicolaides, Phys. Rev. A **55**, 1325 (1997).
- [13] M. E. Goggin and P.W. Milonni, Phys. Rev. A **37**, 796 (1988).
- [14] A. Guldberg and G. D. Billing, Chem. Phys. Lett. **186**, 229 (1991).
- [15] B. Wu and W-K. Liu, Physica A **205**, 470 (1994).
- [16] M. Thachuk and D. M. Wardlaw, J. Chem. Phys. **102**, 7462 (1995).
- [17] C. A. Nicolaides, Th. Mercouris and I. D. Petsalakis, Chem. Phys. Lett. **212**, 685 (1993).
- [18] P. C. Dardi and S. K. Gray, J. Chem. Phys. **77**, 1345 (1982).

- [19] R. Heather and H. Metiu, *J. Chem. Phys.* **88**, 5496 (1988).
- [20] A. D. Bandrauk, E-W. S. Sedik and C. F. Matta, *J. Chem. Phys.* **121**, 7764 (2004).
- [21] S. Huang, C. Chandre and T. Uzer, *J. Phys. B* **40**, F181 (2007); *J. Phys. B* **41**, 035604 (2008).
- [22] R. Bachelard, C. Chandre and X. Leoncini, *Chaos* **16**, 023104 (2006).
- [23] M. Joyeux, S. Yu. Grebenshchikov, J. Bredenbeck, R. Schinke and S. C. Farantos, *Adv. Chem. Phys.* **130**, 267 (2005).
- [24] S. C. Farantos, Z.W. Qu, H. Zhu and R. Schinke, *Int. J. Bifurcation Chaos Appl. Sci. Eng.* **16**, 1913 (2006).
- [25] P. Cvitanović, R. Artuso, R. Mainieri, G. Tanner and G. Vattay, *Chaos: Classical and Quantum*, ChaosBook.org (Niels Bohr Institute, Copenhagen 2005).
- [26] J. M. Greene, *J. Math. Phys.* **20**, 1173 (1979).
- [27] R. S. MacKay, *Nonlinearity* **5**, 161 (1992).

List of Figures

1 Poincaré section of Hamiltonian (2) for $F_1 = 0.18$, $F_2 = 0.02$ and $\phi = 0$. The dot and the cross indicate the elliptic periodic orbit \mathcal{O}_e and its associated hyperbolic one, respectively. The inset depicts a projection of \mathcal{O}_e in the (r, p) plane. 14

2 Action(solid) and angle(dashed) curves for $F_1 = 0.18$ and $F_2 = 0.02$ 15

3 Residue curves (bold solid) for the considered set of periodic orbits for $F_1 = 0.18$ and $F_2 = 0.02$: for \mathcal{O}_e (upper curve) and for \mathcal{O}_h (lower curve). The arrow indicates where the bifurcation happens. 16

4 Contour plots of the residues of \mathcal{O}_e in the (F_1, F_2) plane for (a) $\phi = 0$, (b) $\phi = \pi/6$, (c) $\phi = \pi/2$ and (d) $\phi = \pi$. White dashed curves indicate $R(F_1, F_2) = 1$ where \mathcal{O}_e bifurcates. Two white solid curves in (a) indicate $R(F_1, F_2) = 0$. The small region enclosed by two thin white lines near the up-right corner in (b) corresponds to a region where \mathcal{O}_h is elliptic. Crosses (respectively circles) on panel (a) represent the values of parameters where laminar plots have been computed in Fig. 5 (respectively Fig. 6). 17

5 Laminar plots with $\phi = 0$ for (a) $(F_1, F_2) = (0.1405, 0.025)$, (b) $(F_1, F_2) = (0.1559, 0.04)$ and (c) $(F_1, F_2) = (0.165, 0.055)$. The cutoff time is $200\pi/\omega_1 \approx 2244$ and the energy threshold is $E_{th} = 2$ 18

6 Laminar plots with $\phi = 0$ for (a) $(F_1, F_2) = (0.19, 0.055)$, and (b) $(F_1, F_2) = (0.14, 0.055)$. The cutoff time is $200\pi/\omega_1 \approx 2244$ and the energy threshold is $E_{th} = 2$ 19

- 7 Residue versus F_1 for both elliptic and hyperbolic periodic orbits at $F_2 = 0.03$ for (a) several different values of ϕ : $\phi = \pi/6$ (dash-dotted), $\phi = 0.35$ (solid), $\phi = 0.2$ (dotted) and $\phi = 0.06$ (dashed), and (b) $\phi = 0$ 19

Figures

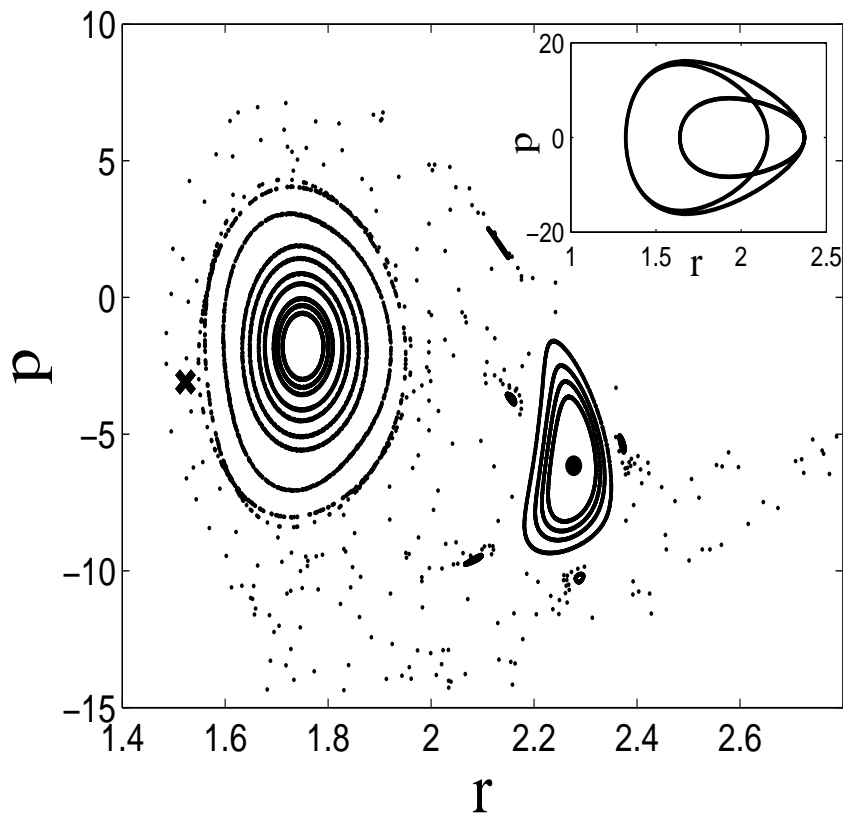


FIG. 1: Poincaré section of Hamiltonian (2) for $F_1 = 0.18$, $F_2 = 0.02$ and $\phi = 0$. The dot and the cross indicate the elliptic periodic orbit \mathcal{O}_e and its associated hyperbolic one, respectively. The inset depicts a projection of \mathcal{O}_e in the (r, p) plane.

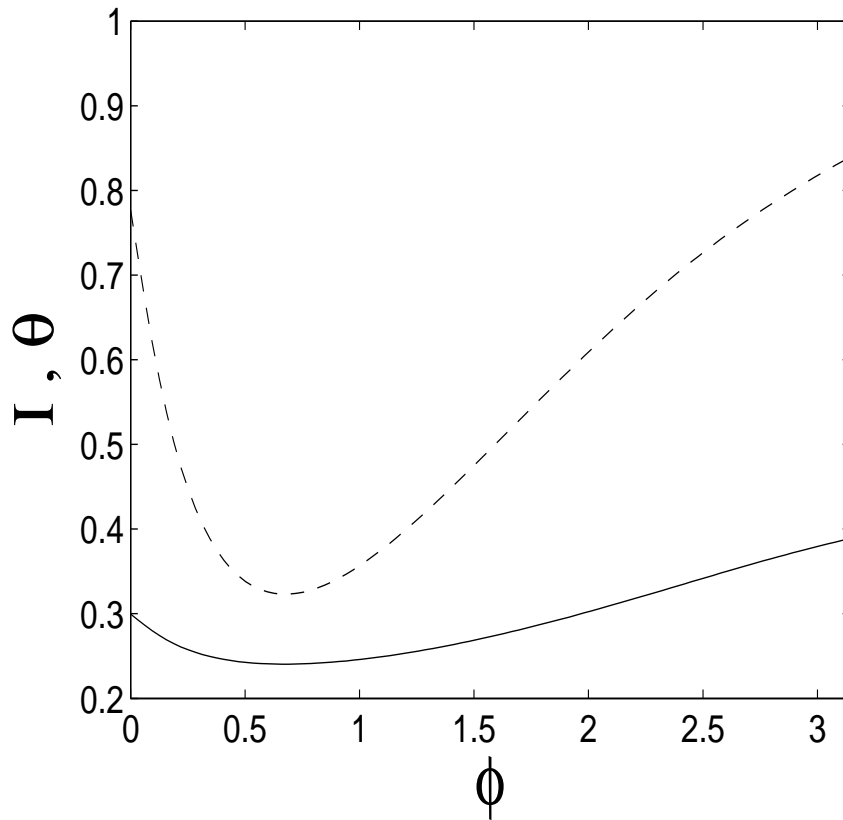


FIG. 2: Action(solid) and angle(dashed) curves for $F_1 = 0.18$ and $F_2 = 0.02$.

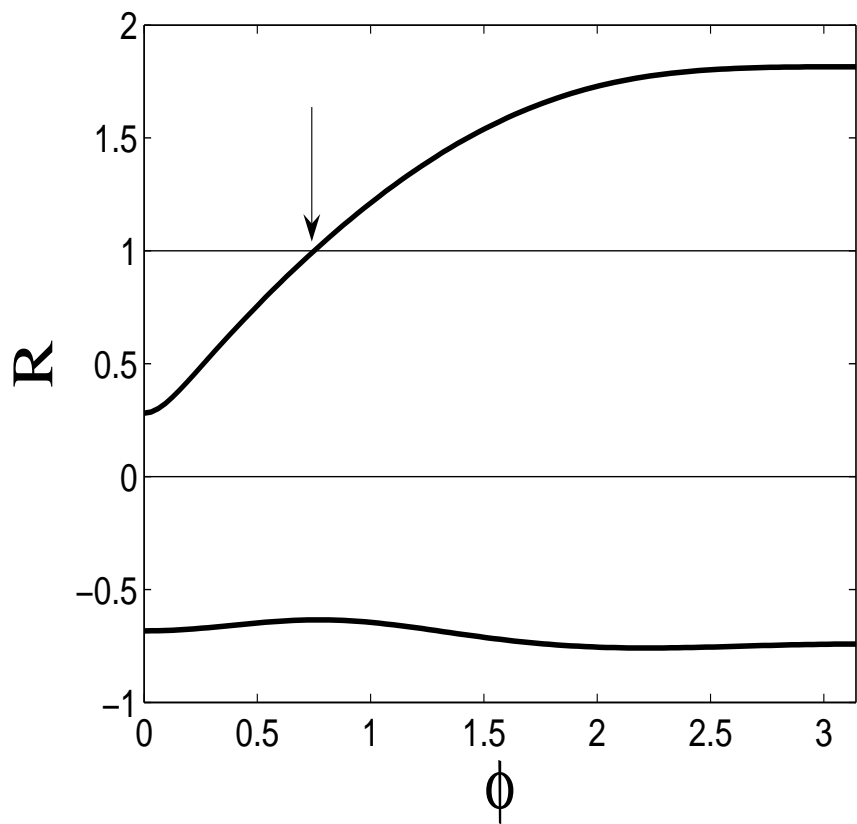


FIG. 3: Residue curves (bold solid) for the considered set of periodic orbits for $F_1 = 0.18$ and $F_2 = 0.02$: for \mathcal{O}_e (upper curve) and for \mathcal{O}_h (lower curve). The arrow indicates where the bifurcation happens.

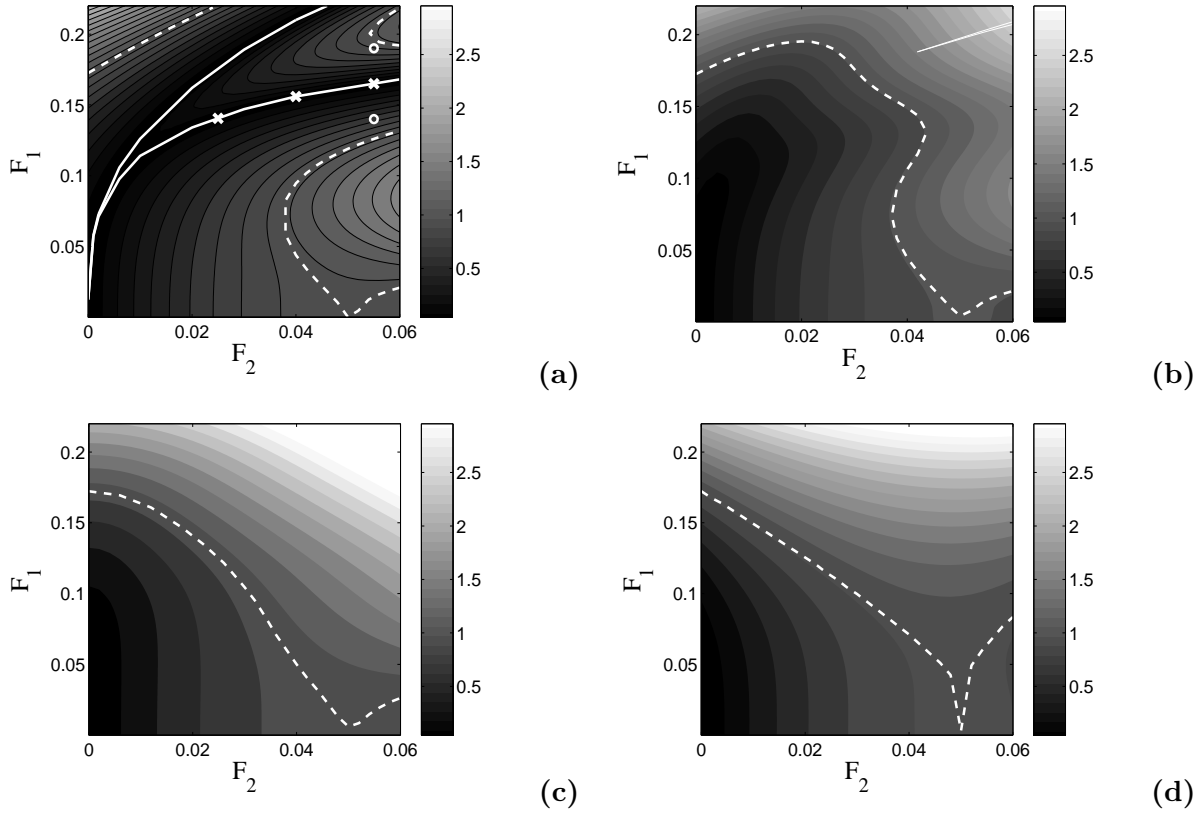


FIG. 4: Contour plots of the residues of \mathcal{O}_e in the (F_1, F_2) plane for (a) $\phi = 0$, (b) $\phi = \pi/6$, (c) $\phi = \pi/2$ and (d) $\phi = \pi$. White dashed curves indicate $R(F_1, F_2) = 1$ where \mathcal{O}_e bifurcates. Two white solid curves in (a) indicate $R(F_1, F_2) = 0$. The small region enclosed by two thin white lines near the up-right corner in (b) corresponds to a region where \mathcal{O}_h is elliptic. Crosses (respectively circles) on panel (a) represent the values of parameters where laminar plots have been computed in Fig. 5 (respectively Fig. 6).

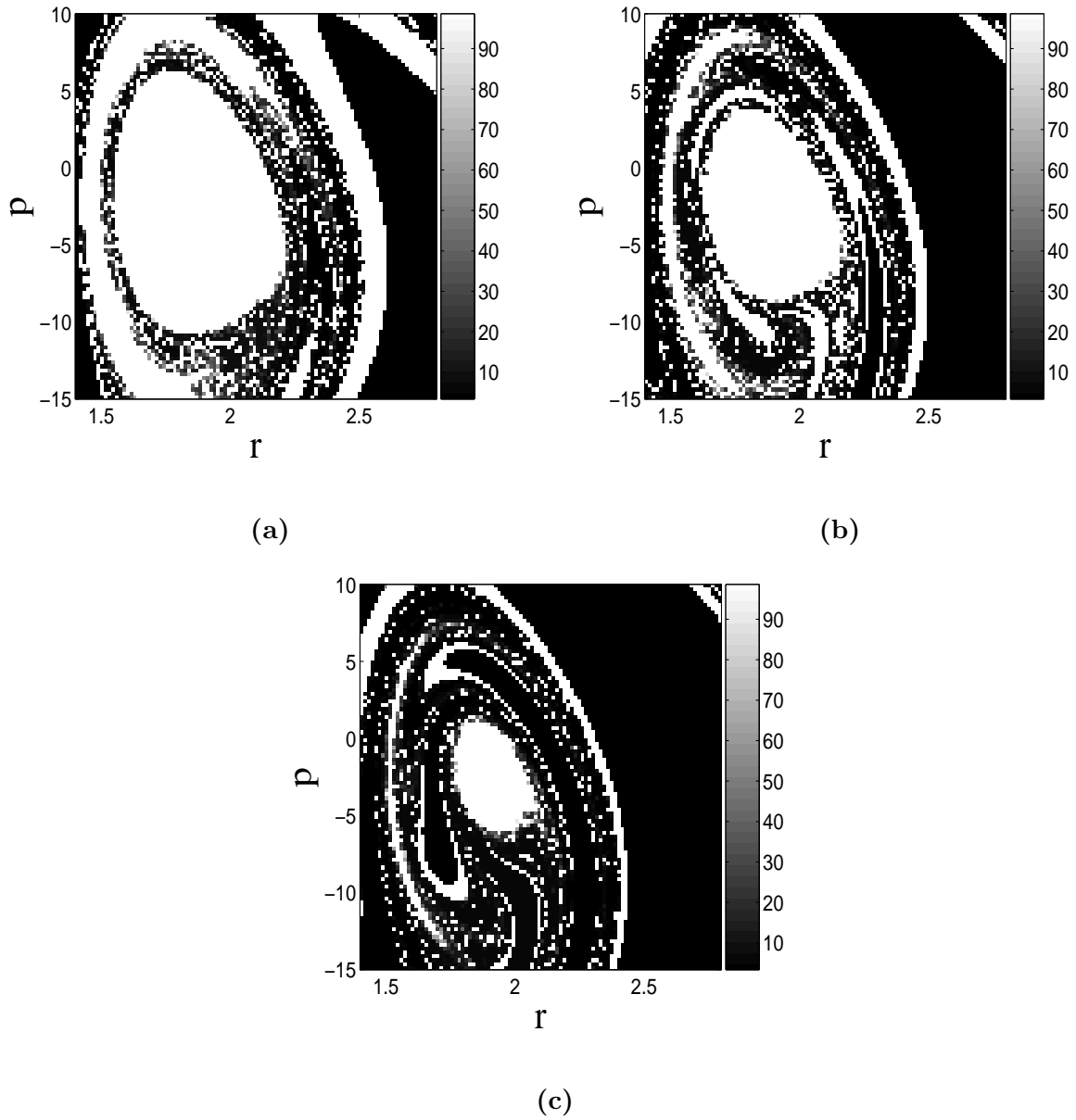


FIG. 5: Laminar plots with $\phi = 0$ for (a) $(F_1, F_2) = (0.1405, 0.025)$, (b) $(F_1, F_2) = (0.1559, 0.04)$ and (c) $(F_1, F_2) = (0.165, 0.055)$. The cutoff time is $200\pi/\omega_1 \approx 2244$ and the energy threshold is $E_{th} = 2$.

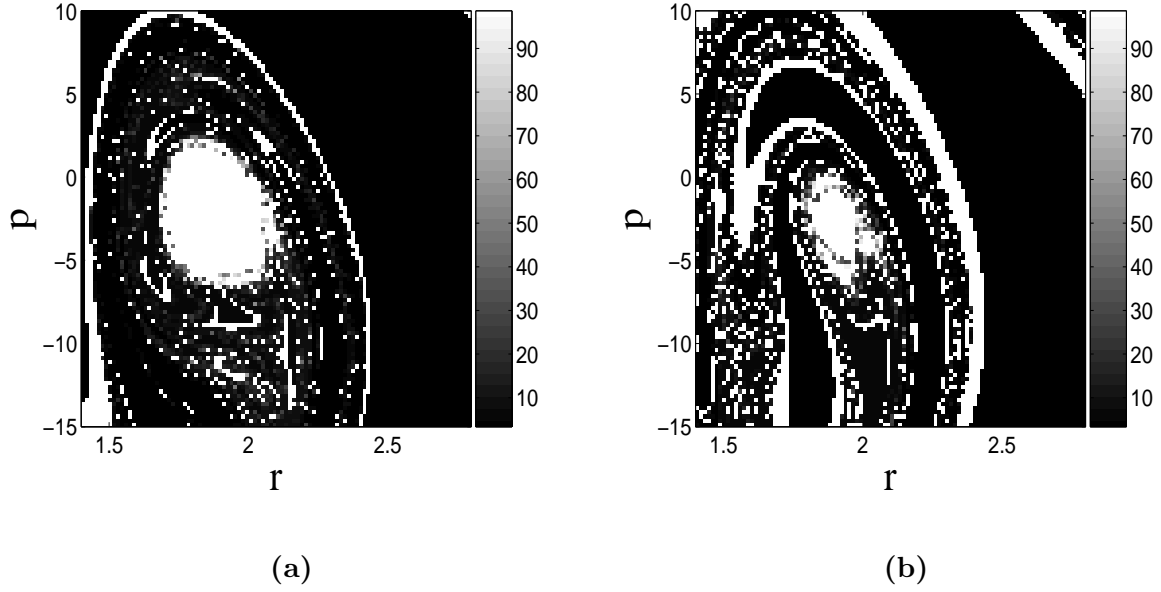


FIG. 6: Laminar plots with $\phi = 0$ for (a) $(F_1, F_2) = (0.19, 0.055)$, and (b) $(F_1, F_2) = (0.14, 0.055)$.

The cutoff time is $200\pi/\omega_1 \approx 2244$ and the energy threshold is $E_{th} = 2$.

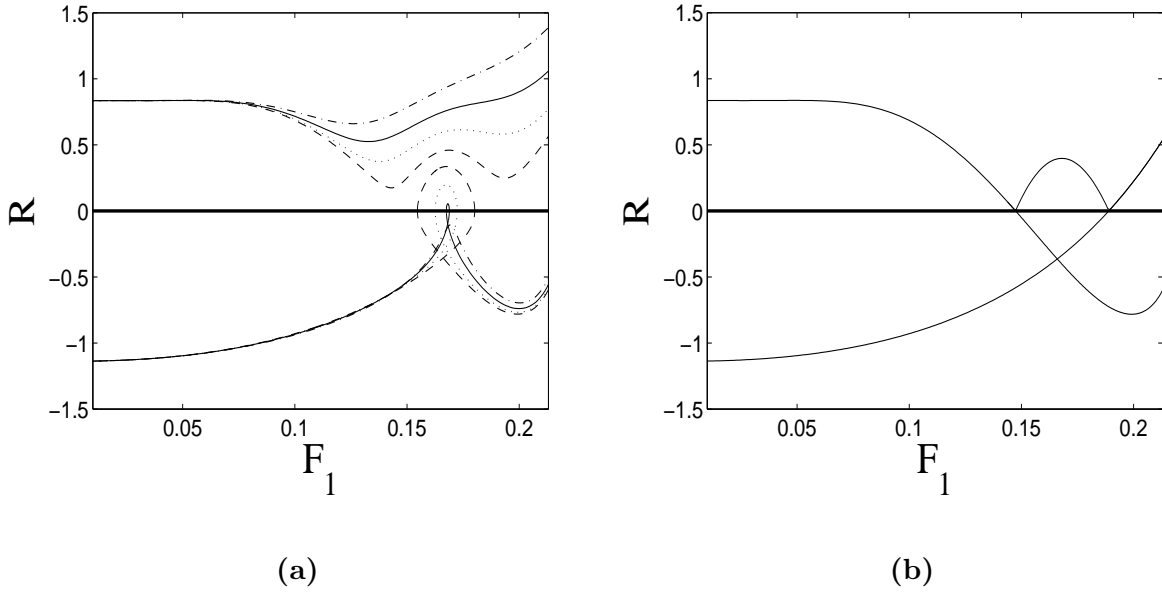


FIG. 7: Residue versus F_1 for both elliptic and hyperbolic periodic orbits at $F_2 = 0.03$ for (a) several different values of ϕ : $\phi = \pi/6$ (dash-dotted), $\phi = 0.35$ (solid), $\phi = 0.2$ (dotted) and $\phi = 0.06$ (dashed), and (b) $\phi = 0$.